A STUDY OF THE INTRODUCTION OF IONS INTO THE REGION OF STRONG FIELDS WITHIN A QUADRUPOLE MASS SPECTROMETER

By
WILSON M. BRUBAKER

BELL & HOWELL RESEARCH CENTER
360 SIERRA MADRE VILLA
PASADENA, CALIFORNIA

CONTRACT NASW-1298

FOURTH
QUARTERLY PROGRESS REPORT
for the period
17 MAY THROUGH 17 AUGUST 1966

NATIONAL AERONAUTICS AND SPACE ADMINISTRATION
WASHINGTON, D. C.

A STUDY OF THE INTRODUCTION OF IONS INTO THE REGION OF STRONG FIELDS WITHIN A QUADRUPOLE MASS SPECTROMETER

by

Wilson M. Brubaker

ABSTRACT

This project is a theoretical and experimental study of the introduction of ions into the strong fields of a quadrupole mass filter. Computer studies have been extended to reveal the manner in which the maximum amplitudes of the trajectories are influenced by the length of the fringing field, in periods of the applied ac potentials. Experimental data reveals that the influence of ion injection energy is different for the conventional and the delayed dc modes of operation. The perturbation of the fields within the quadrupole structure by the substitution of round instead of hyperbolic electrode surfaces has been calculated. Selected trajectories have been computed for the perturbed fields. These trajectories depart markedly from those for corresponding hyperbolic quadrupoles. For the general case, limited progress was made in predicting the influence of the field perturbations upon the trajectories.

TABLE OF CONTENTS

LIST OF TABLES AND FIGURES

Tables

Figures

INTRODUCTION

This report covers the work done by the Bell & Howell Research Center on NASA Contract NASW-1298 from 17 May through 17 August 1966. This is the fourth quarter of the Contract.

This project is concerned with the introduction of ions into the region of strong fields in the quadrupole mass filter. During the preceeding quarters, computer calculations and laboratory experiments have been made. These data combine to indicate that the amplitudes of the trajectory as the ion traverses the filter are strongly dependent upon the manner in which the ion is introduced into the quadrupole.

During the present quarter the computer studies have been extended to show the perturbations of the fields which result from the substitution of round rods for the hyperbolic surfaces. In some instances these perturbations are surprisingly large. As anticipated, their influence is largest in the outer portions of the region occupied by the ions.

The laboratory experiments have been extended to include a wider range of resolving power, entrance geometry, and ion energy.

COMPUTER STUDIES

Fringing Field Considerations, Conventional Quadrupole

In the first quarter, computer studies of the influence of fringing fields upon the trajectories in the conventional quadrupole were given for configurations of varying duration. In particular, trajectories were calculated for ramps of zero, two, and ten cycle lengths. The importance of knowing the dependence of normalized maximum trajectory amplitude upon ramp length has become more apparent during the recent experiments. Therefore, these data have been extended to ramps of other lengths.

As the ions pass from a region where the fields are essentially zero to the position inside the quadrupole where the fields are of essentially full strength, a number of radio-frequency rod excitation cycles occur. This number is given by

$$n_f = (l_f/v_z) f_{MHz}$$

Where l_f is the length of the fringing field in centimeters, f_{MHz} is the excitation frequency in mega-Hertz, and v_z is the axial ionic velocity in centimeters per microsecond.

During the passage of ions through the fringing field, the working point in the stability diagram moves from the origin to the vicinity of the apex, along a path which lies almost entirely outside the stable region. As discussed in earlier reports, this passage through the fringing fields causes the ions to receive very large impulses in the positive y-direction, resulting in trajectories with amplitudes much larger than the apparatus. (These ions of course, are not transmitted through the quadrupole.)

The data presented in Figure 1 relate maximum trajectory amplitude to ramp length at a resolving power of approximately one hundred. The points fall very near to a straight line, whose equation is given by

$$A_{max} = 3.5 \times 10^{0.25n} \qquad n \geq 2$$

According to theory, the maximum amplitude is proportional to the square root of the resolving power. Since the above equation was calculated for a resolving power of 100, the general equation becomes

$$A_{max} = 0.35\ (\text{Resolving Power})^{1/2} \times 10^{0.25n}$$

That the maximum amplitude should vary exponentially with time spent by the ion in the fringing fields could have been expected. Simple theory

relates the acceleration experienced by the ions to the vertical distance between the working point and the stability limit. When the working point is above the stability limit, the acceleration is positive and the ions move into ever-increasing fields. Under this condition the trajectories increase exponentially with time. Since the distance between the working point and the stability limit changes continuously as the ions traverse the fringing field, the exponential relationship for the maximum amplitude was not apparent before the calculations were made.

The above data indicate the importance of minimizing the number of cycles spent by the ions in the fringing field of the conventional quadrupole.

Derivation of Potentials and Fields, Round Electrodes

The computer has been used to determine the potentials in the quadrupole when the field-forming surfaces are round rods. In particular, it has been used to determine the fields for the case of rod radius equal to 1.16 times the instrument radius, r_o. This is the compromise rod radius which has been most commonly used. Lines representing contours of the round and the hyperbolic surfaces touch in three places for each electrode: on the axis, and at symmetrical points which lie at the intersections of the circle and radii at angles of about 32.5° relative to the x- or y-axis. This particular compromise causes the fields near the instrument axis to be very similar for equal excitation potentials on the round and hyperbolic electrodes.

Last month's report described the relaxation method used for the determination of the potentials. From a knowledge of these potentials the x- and y-components of the fields have been derived. Since ions respond to fields and are uninfluenced by potentials, the results of these calculations are presented as perturbations (fractional deviation) of the fields.

The data of the perturbation of the fields as a function of position in the plane perpendicular to the instrument axis are presented in Figures 2 to 3 and in Table I. From symmetry, x and y are interchangeable.

The data presented relate the fields to positions in the x-y plane. This field variation is equivalent to a variation in the a-q values over the x-y plane, as is shown below:

$$V = (V_{dc} + V_{ac} \cos \omega t)\ (x^2 - y^2)/r_o^2$$

$$E_x = (-2x/r_o^2)\ (V_{dc} + V_{ac} \cos \omega t)$$

$$= (-m\omega^2/4e)\ (a + 2q \cos \omega t)\ x$$

Similarly,

$$E_y = (m\omega^2/4e)\ (a + 2q \cos \omega t)\ y.$$

Since these fields are supported by potentials on a single set of electrodes, the ratio of a/q is constant over the entire x-y plane. Thus, a variation of the fields as a function of position in the x-y plane is equivalent to a proportionate variation in a and q.

Trajectories in Perturbed Fields, General Comments

When the fields in the quadrupole are the result of potentials applied to hyperbolic surfaces, the equi-potential surfaces throughout the instrument are themselves hyperbolic. However, when round rods are used in the place of hyperbolic surfaces, the equi-potentials depart slightly from hyperbolae. It is the purpose of this investigation to evaluate these departures. The departures are described as fractional variations (perturbations) of the fields from those which result from the use of hyperbolic rod surfaces.

The trajectories computed in this present study were made under conditions quite different from those previously discussed where attention was focused on the passage of ions through the fringing field at the entrance to the quadrupole. Here the entrance to the quadrupole is completely ignored; the ions are assumed to be within the quadrupole where the fields have full strength. The velocity vector is entirely radial, so the ions never enter or leave the quadrupole. In many of the computations the initial radial velocity is the independent parameter of a family of curves.

In the computation of the ionic trajectories the previously obtained information of the field perturbations was used. The independent variable is the velocity with which the ions enter the radial fields. The instrument radius, r_o is normalized to unity. The initial velocity of the ions is given in units of r_o per microsecond, and the time axis is in radians of the applied ac potentials. The specification of the a-q values sets the ratio of the applied dc and ac potentials, but does not determine their absolute values.

Consistent with obtaining the maximum amount of information in the least time and expense, the computer was asked to print out only the envelopes of the trajectories. In many instances, the computations were interrupted when it was obvious that the maximum amplitude of the envelope had been passed.

As is so well shown by the solutions of the Mathieu equation in which the a-q diagram is divided into regions of stability and those of instability,

the nature of the ionic trajectories is determined by the a-q values of the working point. Since the working point lies very close to the stability limits when the quadrupole is being used at high resolving powers, very small changes in the a-q values can have a profound effect upon the trajectories.

The description of the dependence of the trajectory upon the position of the working point usually assumes that the locus of the working point is the same for all values of x and y. When the locus of the working point becomes x- and y-dependent, the situation becomes very complicated, because the ions execute rapid excursions over large portions of the x-y plane. Obviously, the envelope of the trajectories is influenced by the integrated effect of the forces as the ions move over the x-y plane and experience regions of varying a-q values. However, even when the x- and y-components of the fields, or their equivalent a-q values are known over the x-y plane, it is not easy to predict the nature of the resulting ionic trajectories. In later sections of this report an attempt is made to correlate the distortion of the usual trajectory envelopes with the calculated field perturbations.

A glance at the plot of the field perturbations (Figures 2 and 3) reveals that there is no such thing as a typical trajectory which can be considered for the purposes of comparing the operation of round and hyperbolic rod quadrupoles. In the round rod case the y-component of field is dependent not only upon the y-position, but also upon the x-position. In the hyperbolic case the y-component of field is completely independent of the x-position, and the "y-trajectories" are the same for all values of x.

The general characteristics of the y-trajectories are well understood without resort to the solutions of Mathieu's equation, as described in the First Quarter's Report. However, the x-trajectories are not similarly appreciated. Thus it follows that it is easier to interpret the influence of the field perturbation for the y-trajectories than it is for the x-trajectories.

The conditions under which the trajectories were calculated are such that the fields near the instrument axis are the same for both shapes of field-forming surfaces. Hence, for amplitudes which lie near the instrument axis there is negligible difference between the trajectories in the two cases. Because the fields near the axis are quite small (zero on the axis) they do not have as great an influence on the trajectories as do the fields remote from the axis. In general, the perturbations in the fields produced by the round rods increase rapidly with the distance from the axis. Since ions spend more time at positions remote from the axis than at positions close to the axis, the importance of the perturbations

becomes apparent. The perturbations on the x- and y-axes increase slowly from zero on the instrument axis to a maximum value at the rods. In other planes the perturbations vary with position in a much more complicated manner.

If the incremental change in the a-q values occurred all over the x-y plane, the influence on the trajectories would be apparent. Weakening of the fields is equivalent to a motion of the working point in the stability diagram toward the origin. To the extent that the effect of this decrease in the a-q values can be simply interpreted, it corresponds to an increase in the stability of the x-component of motion, and a lessening of the stability of the y-component.

The case under consideration is not as simple as that just discussed, because the ions oscillate in response to the applied field, and thus are not responsive uniquely to the values of the fields at a particular point. Rather, the ions travel over a considerable portion of the x-y plane. Further, as far as the y-component of motion is concerned, any weakening of the fields at the maximum excursion of the ionic position during any ac cycle appreciably weakens the average acceleration of the ion toward the instrument axis. Similarly, any strengthening of the fields at the outer excursion of the trajectory tends to increase the acceleration of the ion toward the axis. Our present understanding of the x-component of motion permits interpretation of the influence of the perturbations only in terms of the position of the working point in the stability diagram. That is, a weakening of the field increases the stability, and vice versa.

Regardless of the detailed nature of the x- and y-trajectories, the envelopes to the traces are sine waves for the hyperbolic rod quadrupole. The particular working points in the stability diagram used for computations were chosen to make the periods and amplitudes of the envelopes nearly identical for the x- and y-components of motion. Through an observation of the distortion of the envelopes from their normal sinusoidal form an estimate of the influence of the field perturbations may be obtained.

Y-Trajectories in the Perturbed Field

In its response to the y-component of electric field, the ion oscillates in near synchronism with the applied ac field, with a peak-to-peak amplitude which is half the maximum excursion from the x-z plane. For the hyperbolic case the value of the maximum amplitude (envelope) varies sinusoidally with time. This characteristic is displayed in the normal hyperbolic trajectory of Figure 4. When the excursion of the trajectory penetrates to regions where the field perturbation becomes appreciable, the nature of the trajectory is changed. This change is noted first as a variation in the period of the trajectory envelope.

The y-component of motion of the ions is characterized by a near balance between two large, oppositely-directed accelerations. The field which results from the dc potential applied to the rods accelerates the ions toward the rods, away from the axis. Except that the opposing acceleration which results from the motion of the ions in non-uniform fields exceeds that due to the dc field, the ions continue their radial y-directed motion and strike the rods. The restoring influence of the motion of the ions in the ac field results from the larger magnitude of the field at greater y-distances.

One potentially effective manner of evaluating the distortion of the envelope is to calculate the acceleration from its curvature. For the hyperbolic case, where the envelope is a sine wave, the acceleration is proportional to the displacement. The constant of proportionality is logically termed the "acceleration constant", in a manner similar to that of the "spring constants" of force equations. When the contour of the envelope is not sinusoidal, the "acceleration constant" is no longer constant, but it becomes a function of the displacement. The differential equation of the envelope then becomes

$$\ddot{y} = -k(y)\ y$$

If this equation is solved for k(y),

$$k(y) = -d(v_y)/(ydt)$$

k(y) can be evaluated from the envelope contour data by observing the change in the velocity at a given displacement in a small interval of time.

The data from the computer contain the maxima of the high frequency excursions of the ions. These form points on the trajectory envelope, and can be used to calculate k(y) as described above.

Y-trajectories were computed at two resolving powers: 100 and 400. In the data for the lower resolving power the critical value of the injection velocity which causes ions to strike the rods was well determined. In Figure 4 it is seen how a very small change in the initial velocity of the ion causes its trajectory to change abruptly from one of bounded amplitude to one of an ever-expanding amplitude. This change occurs at a normalized radial distance of 0.82 r_o. As discussed above, k(y) becomes zero at this value of y, and reverses sign for values of y larger than 0.82 r_o.

Similar trajectory envelopes for the y-component of motion at a higher resolving power of 400 (and for x = 0) are shown in Figure 5. Most impressive is the observation that the ion trajectory becomes unstable at a

y-value of only 0.67 r_o, instead of 0.82 r_o as it was for the lower resolving power case. Values of the normalized acceleration, k(y), were calculated from these data. The results are presented in Figure 6. For small values of y, the computed values of k(y) scatter about the constant value of the hyperbolic case. For values of y greater than 0.67, it is seen that k(y) becomes strongly positive, indicating that the ion is being accelerated outward at a high rate. If the values of a and q were nearly constant over the interval in y represented by the peak-to-peak values of y, then the perturbation of the trajectory envelope could be well correlated with a shift of the working point in the stability diagram. Unfortunately, this is not the case. The shift in the locus of the working point during one cycle of the applied potential is in many cases sufficient to carry it outside the stability diagram. When such large excursions occur, it is necessary to consider the accelerations which the ions receive during the entire cycle of applied voltage. Because the perturbations depend upon the x-y position in such a peculiar way, and because the complex motions of the ions carry them over the entire x-y plane in a manner which is highly dependent upon the exact position of the working point in the stability diagram (along the scan line), it is not possible to correlate the trajectory envelopes with the details of the field perturbations in a very precise manner.

The trajectory envelopes of Figure 5 were computed for a-q values which would give resolving powers of about 400. It is interesting to observe the perturbations of the E_y field for x = 0, as they relate to this situation. Were the incremental change in the a-q values the same all over the x-y plane, it would need to be of the order of dm/(2m) to scan a half peak width, as is required to go from the peak to the valley. This is a value of 0.00125. Surprisingly, the trajectory becomes unstable when only the outermost excursion of it, as given by the envelope, reaches a region where the perturbation is 0.0011. When the ion is at its maximum excursion of 0.67 r_o, its associated minimum excursion is about 0.34 r_o. At this value of y the perturbation is 0.00023. Thus it is seen that over the space reached by the ion in one cycle of its motion the perturbation is very much less than that required to render the trajectory unstable if the perturbation were everywhere the same.

That the relatively small average perturbation of the fields renders the trajectory unstable results from the nature of the dependence of the perturbation upon the position of the ion. When the ac field at maximum excursion is reduced by the perturbation, this weakens the acceleration toward the axis. It follows that the stability of the trajectory in the perturbed field is influenced not only by the magnitude of the perturbation, but also by the slope of the perturbation as a function of position from the median plane. (Instrument axis for x = 0.)

An example of the dominance of the slope of the perturbation vs. position curve over the value of the perturbation is seen in the y-trajectories in the plane $x = r_o$. Trajectories calculated for different initial velocities are shown in Figure 7. The best measure of the influence of the perturbation is to be found in the time required for a half-period of the trajectory envelope. As reference, for the hyperbolic case the time required for a half-period is 138 radians. For an ion injected at a modest radial velocity of 0.0236 r_o/μsec, the half-period is 25 radians. An initial velocity of 0.0574 results in a half-period of 16 radians, and a velocity of 0.1 results in a half period of 14.5 radians. Compared to operation with hyperbolic rods, the time required for the half-period is reduced by a factor approaching ten and the maximum amplitudes of the trajectories are similarly reduced. As is seen in Figure 3 the perturbation in the y-field for small values of y is very large, and the slope is quite steep. The fact that the ion is so strongly focused toward the axis when the working point lies so far outside the stability limit for the major portion of the trajectory clearly demonstrates the dominance of the slope of the perturbation vs. position over the location of the working point.

The above discussion emphasizes the virtual impossibility of predicting in any detail the nature of the trajectories as a function of the field perturbations. While emphasis has been placed upon the nature of the y-trajectories, similar behavior was seen for the x-trajectories. If the dependence of the trajectories upon the perturbations were all as simple as those for y at $x = 0$, some rather definite predictions could be made. Here it is seen that the ions cannot be made to approach the round electrode on trajectories which return them to the axis. If the trajectory reaches a value of y which is only $(2/3)r_o$ the ion is lost to the rod (for a resolving power of 400). If this were true for most of the trajectories, the advantages of the hyperbolic rods over the round ones would be apparent, and the savings of power through the use of the hyperbolic rods would be very appreciable, since the power increases as the instrument radius to the fourth power.

In some cases, as a function of the trajectory excursion, the perturbations seem to either increase or decrease the stability of the trajectory. In order to predict from computed trajectories the influence of the perturbations, many more trajectories would need to be analyzed than can be accomplished within the available time on this project.

It can be concluded that this study of the trajectory perturbations introduced by the use of round rods reveals disturbing departures from the normal trajectories of the hyperbolic quadrupole. It will be surprising if the laboratory tests of the round and hyperbolic instruments do not reveal a real superiority of the hyperbolic quadrupole over the round one.

EXPERIMENTAL STUDIES

Experimental Apparatus

The main experimental refinement made during this quarter has been the observation of the sensitivity in absolute terms, namely, amperes per torr of the observed peak. To this end the three-inch round rod quadrupole shown in Figure 1 of last quarter's report has been used to monitor the krypton pressure. The calibration of the quadrupole was made daily by observing the incremental changes of the readings of the ion gauge and the quadrupole.

Another significant change is the location of the ion source. It has been moved nearer to the quadrupole. The new entrance geometry is shown in Figure 8. This is to be compared with the geometry of Figure 3 of the Third Quarter's Report.

Experimental Data

Data were obtained at three ion injection energies. The sensitivity in amperes per torr of krypton mass 84 peak is plotted as a function of the resolving power and presented in Figures 9 to 11. The data have been extended over a larger range of the variables during the current quarter.

As the continued refinements resulted in higher resolving power, the importance of the influence of the ion injection energy upon the performance became apparent. Accordingly, runs were made over wide variations in resolving power with different ion injection energies. These studies are being continued, and the initial results are presented in this report. Data have been obtained for operation at 1.6 MHz for ion injection energies of 4, 6, and 15 volts for the conventional and the delayed dc ramp modes of operation.

Figure 9 presents the observed resolving power computed at the 10% peak height level for the conventional quadrupole with ion injection energies of 4, 6, and 15 volts. The strong attenuation of the sensitivity at the lower ion energies is largely the result of the adverse influence of the fringing field. A small part of it is due to a lower source efficiency at the lower accelerating potentials. It is probable that 15 volts is not the optimum injection energy. More data will be obtained, using a wider range of ion injection energies.

Figure 10 shows similar data for operation of the quadrupole in the delayed dc mode. The greater sensitivity of the instrument for 15 volt

ions at low resolving power is more than the suspected increase in source efficiency. The higher resolving power capability of the quadrupole for ions of lower injection energy is quite apparent.

In Figure 11 a comparison is made between the best performance observed in each of the two modes of operation, using the ion injection energy which gave the best results in each case. The variation in sensitivity observed at low resolving power is largely due to the variation in source efficiency at the different ion energies.

A summary of the resolving powers obtained during the past two quarters of operation is presented in Table II. The experimental results are to be compared to the predicted or theoretical values. The Table contains two predicted values; that given empirically by Paul, and that predicted by Brubaker and realized in the monopole, which has the identical fields.

Of particular interest is the high value of the limiting resolving power obtained with an ion injection energy of 4 volts. A resolving power of over 600 at the 10% level was obtained at an excitation frequency of 1.6 MHz. This exceeds the highest resolving power (at the 10% level) reported last quarter for operation at 2.5 MHz. Since the power dissipated in the coil used to resonate the circuit varies as the fifth power of the frequency, the power levels at 2.5 and 1.6 MHz differ by a factor of nine! Thus, it appears that the delayed dc ramp mode of operation is particularly useful for operation at low power levels and high resolution.

ION INJECTION ENERGY CONSIDERATIONS

Different aspects of the influence of the ion injection energy have been mentioned in other parts of this report. The computer study of the detrimental effect of having a large number of ac cycles occur during the ions' transit of the fringing field has been presented. Similarly, the limit of the resolving power imposed by having too few cycles occur during the transit of the spectrometer is well known.

For the case of the conventional quadrupole, it is desirable that the number of cycles spent in the fringing field be kept low, less than two or three. On the other hand, the demands of resolving power may make this impossible. Thus, consistent with the required resolving power, there is an optimum injection energy for a given quadrupole excited at a fixed frequency. Making the quadrupole longer increases the number of cycles spent in transit without changing the number spent in the fringe field and is one possible solution to this problem.

For the case of the delayed dc ramp quadrupole, the lower limit of injection energy is not set by fringing field loss considerations. When it is realized that the only reason for making the quadrupole long is to provide a larger number of cycles for the ion to spend in the mass resolving section, it becomes apparent that with the delayed ramp variation there exists the possibility of making the quadrupole much shorter. The resultant saving in excitation power is somewhat less than the proportional decrease in the length. The lower limit to the energy of the incident ions probably is determined by space-charge-induced potentials in the ion source. This is seen in the lowered sensitivity at low resolving power at the lower ion injection energies in the plot of Figure 10.

DESCRIPTION OF THE NEW QUADRUPOLE SYSTEM

Mechanical

Two new quadrupole systems, which will be made available, include new identical ion sources and detectors. They will be mounted parallel and closely adjacent to each other on a common ion pumped vacuum system. The reason for fabricating two new systems is to have them identical in every respect possible with the exception of the contours of the field-forming surfaces. It will be possible to interchange the rods without disturbing other parameters. Each rod will have an insulated segment at the entrance end. RCA Type C 70120E venetian blind secondary emission multipliers will be used as the detectors. These will have the voltage dividing resistors (Victoreen type RX3) mounted directly on the multiplier cage, within the vacuum system. Provision will be made for these different modes of operation: (a) A conventional ion collector and electrometer; (b) A secondary emission multiplier and electrometer; (c) A secondary emission multiplier with the output displayed directly on an oscilloscope. Each of these modes will be available by a simple switching arrangement.

Fabrication of the new system is nearly complete. Assembly will follow promptly.

Electrical

The new electronic apparatus is shown in block form in Figure 12. It has been designed with special emphasis on the stability of all parameters which influence the performance of the system. The design goals are based partly on theory and partly on experience.

The short term stability in the excitation frequency is expected to exceed one part in 10^6, and that for the dc rod potentials (and the dc/ac voltage ratio) one part in 10^5. The frequency stability is obtained by the use of a crystal controlled oscillator, and the voltage stability by the use of negative feedback around high gain operational amplifiers.

Convenience features include mass setting which is independent of mass scan width, and mass scanning which may be positive, negative, or triangular. Spectral display is voltage-based for the x-y plotter and for the oscilloscope.

CONCLUSIONS

Computer studies of the field perturbations which result from the substitution of round field-forming electrodes in the place of the hyperbolic ones reveal surprisingly large deviations from the assumed fields. Attempts to correlate the perturbation data with the observed trajectories in the perturbed fields were unrewarding. During even a single cycle of the applied ac potentials the ions move through positions of greatly varying perturbations.

Experimental data continue to indicate the superiority of the delayed dc ramp mode of operation over that of the conventional quadrupole. During the present quarter higher resolving power was observed with excitation at 1.6 MHz than was previously reported at 2.5 MHz. Operation at 1.6 MHz requires only 11% as much excitation power as does operation at 2.5 MHz! The use of the delayed dc ramp appears to be particularly important for applications where economy of power is of great importance.

NEXT QUARTER'S ACTIVITIES

Because ion injection energy has been shown to be of such prime importance, and since the optimum injection energy is different for the conventional and the delayed dc ramp modes, its influence will be further explored.

Ion source studies will be started. It is anticipated that a very considerable increase in sensitivity can be obtained from this endeavor.

The apparatus for comparative studies of quadrupole performance with round and hyperbolic rods will be assembled and set into operation. The computer studies of the present quarter indicate that there may be a real saving in the power requirements of the two instruments for comparable performance capabilities.

TABLE I

E_y PERTURBATIONS AT VARIOUS x AND y

y/x	0.1	0.2	0.3	0.4	0.5	0.6	0.7
0.0	-.00000029	-.00000468	-.00002434	-.00008244	-.00022995	-.00058669	-.00143147
0.1	.00000116	.00000556	.00000242	-.00002304	-.00009821	-.00029027	-.00077210
0.2	-.00001176	.00001809	.00005551	.00009946	.00017511	.00034362	.00069667
0.3	-.00009274	-.00001246	.00008132	.00017382	.00032312	.00071885	.00174580
0.4	-.00035969	-.00015287	.00005997	.00017093	.00018380	.00032633	.00116691
0.5	-.00111688	-.00055384	.00003325	.00028714	-.00001105	-.00076404	-.00141202
0.6	-.00319634	-.00168890	.00000812	.00100335	.00057639	-.00153666	-.00497809
0.7	-.00873912	-.00494287	-.00038011	.00298774	.00346805	.00013517	-.00697810
0.8	-.02284181	-.01385659	-.00260809	.00680168	.01085148	.00753379	-.00342518
0.9	-.05696569	-.03664422	-.01068985	.01239948	.02561574	.02524696	.01102738
1.0	-.13611959	-.09131313	-.03383776	.01846086	.05176245	.05979041	.04338418

TABLE I

E_y PERTURBATIONS AT VARIOUS x AND y

y/x	0.1	0.2	0.3	0.4	0.5	0.6	0.7
0.0	-.00000029	-.00000468	-.00002434	-.00008244	-.00022995	-.00058669	-.00143147
0.1	.00000116	.00000556	.00000242	-.00002304	-.00009821	-.00029027	-.00077210
0.2	-.00001176	.00001809	.00005551	.00009946	.00017511	.00034362	.00069667
0.3	-.00009274	-.00001246	.00008132	.00017382	.00032312	.00071885	.00174580
0.4	-.00035969	-.00015287	.00005997	.00017093	.00018380	.00032633	.00116691
0.5	-.00111688	-.00055384	.00003325	.00028714	-.00001105	-.00076404	-.00141202
0.6	-.00319634	-.00168890	.00000812	.00100335	.00057639	-.00153666	-.00497809
0.7	-.00873912	-.00494287	-.00038011	.00298774	.00346805	.00013517	-.00697810
0.8	-.02284181	-.01385659	-.00260809	.00680168	.01085148	.00753379	-.00342518
0.9	-.05696569	-.03664422	-.01068985	.01239948	.02561574	.02524696	.01102738
1.0	-.13611959	-.09131313	-.03383776	.01846086	.05176245	.05979041	.04338418

TABLE I

(Continued)

y/x	0.8	0.9	1.0
0.0	-.00338361	-.00775858	-.01726971
0.1	-.00195841	-.00476961	-.01113831
0.2	.00132995	.00229549	.00354503
0.3	.00407009	.00879848	.01782870
0.4	.00376013	.00988997	.02255127
0.5	-.00080254	.00298152	.01293319
0.6	-.00872107	-.01108692	-.00977048
0.7	-.01698273	-.02842574	-.03968212
0.8	-.02095677	-.04335915	-.06907258
0.9	-.01494124	-.04968874	-.09067999
1.0	.00761013	-.04144051	-.09883717

TABLE II

THEORETICAL AND EXPERIMENTAL RESOLVING POWERS

Excitation Frequency	Ion Energy	Resolving Power				Quarter Observed
		Paul	Theory	Observed		
				Conventional	Delayed	
1.6	15	180	540	244	270	Third
2.5	15	440	1320	360	560	Third
1.6	4	670	2010	250	630	Fourth
1.6	6	450	1350	400	500	Fourth
1.6	15	180	540	380	380	Fourth

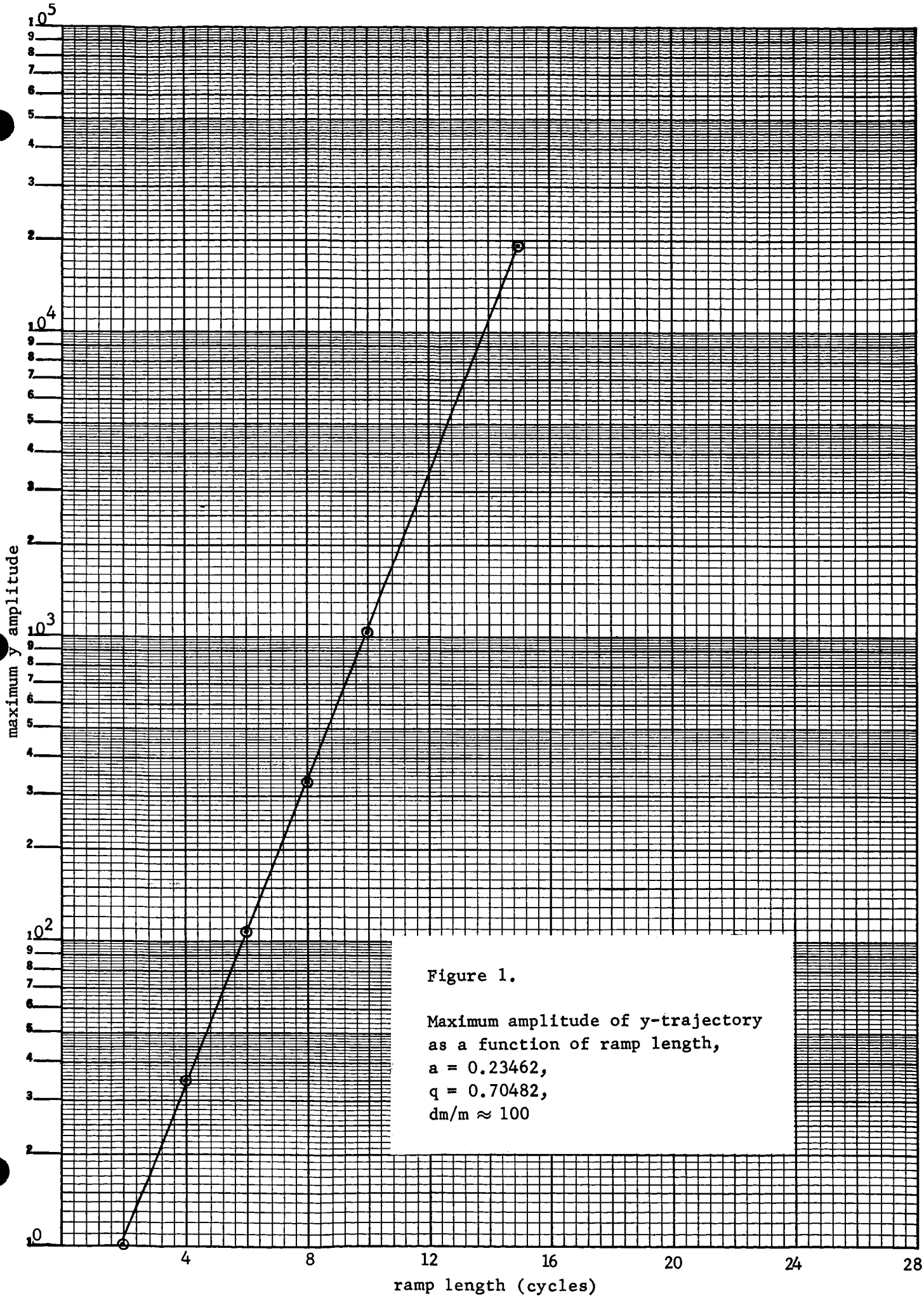

Figure 1.

Maximum amplitude of y-trajectory as a function of ramp length,
a = 0.23462,
q = 0.70482,
dm/m ≈ 100

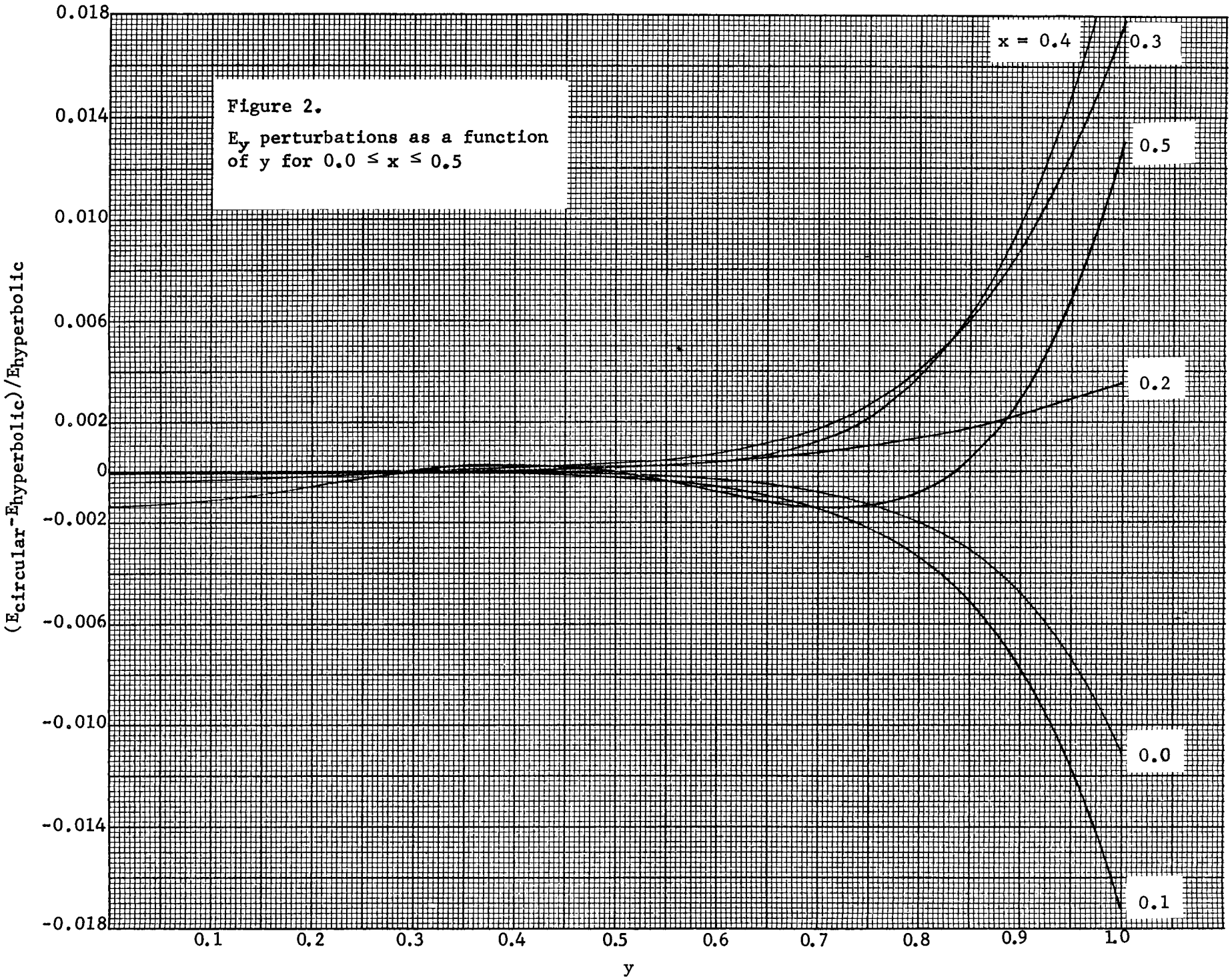
Figure 2.
E_y perturbations as a function of y for $0.0 \leq x \leq 0.5$
$(E_{circular} - E_{hyperbolic})/E_{hyperbolic}$
0.018
0.014
0.010
0.006
0.002
0
-0.002
-0.006
-0.010
-0.014
-0.018
0.1
0.2
0.3
0.4
0.5
0.6
0.7
0.8
0.9
1.0
y
x = 0.4
0.3
0.5
0.2
0.0
0.1

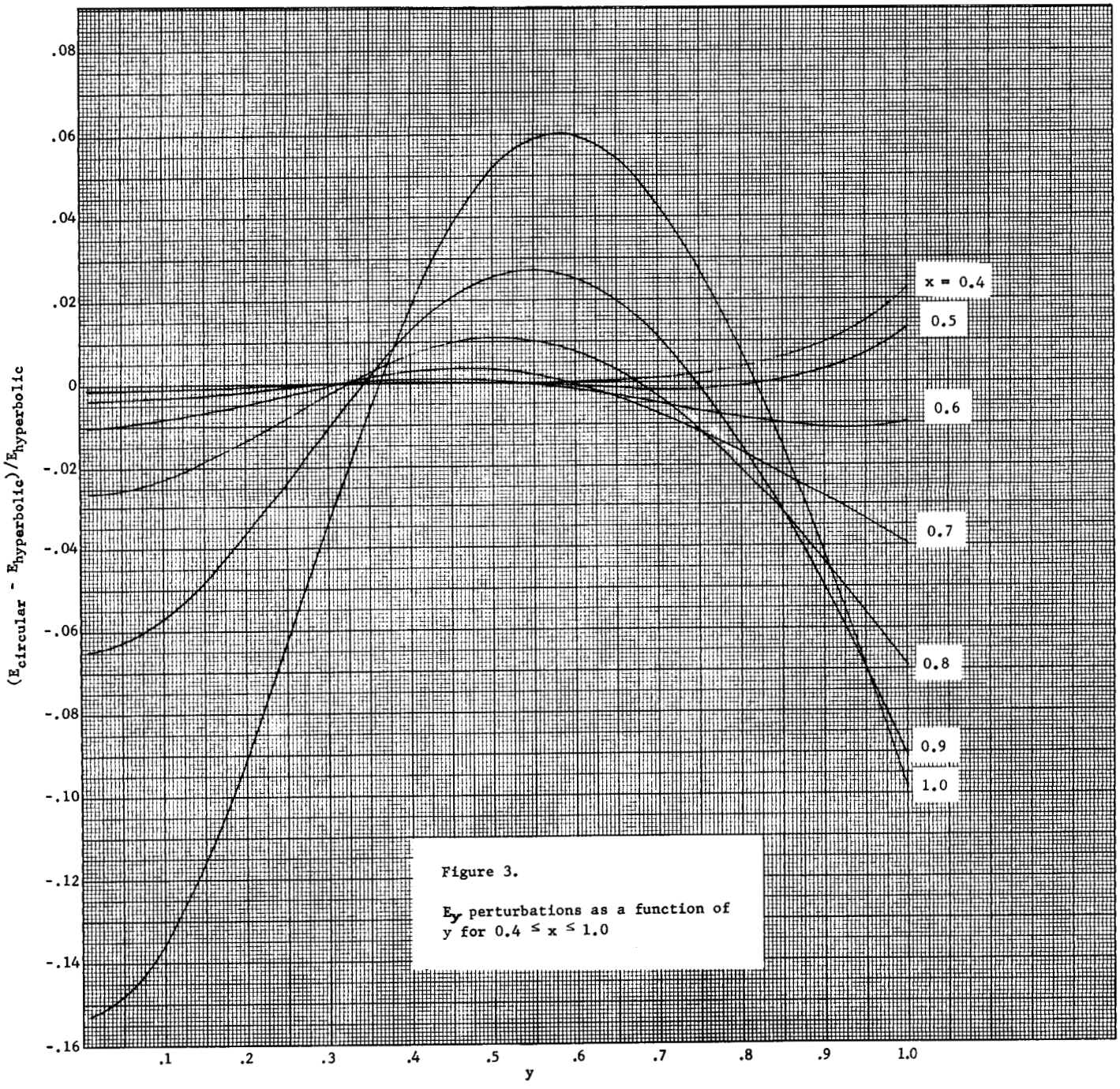

Figure 3.

E_y perturbations as a function of y for $0.4 \leq x \leq 1.0$

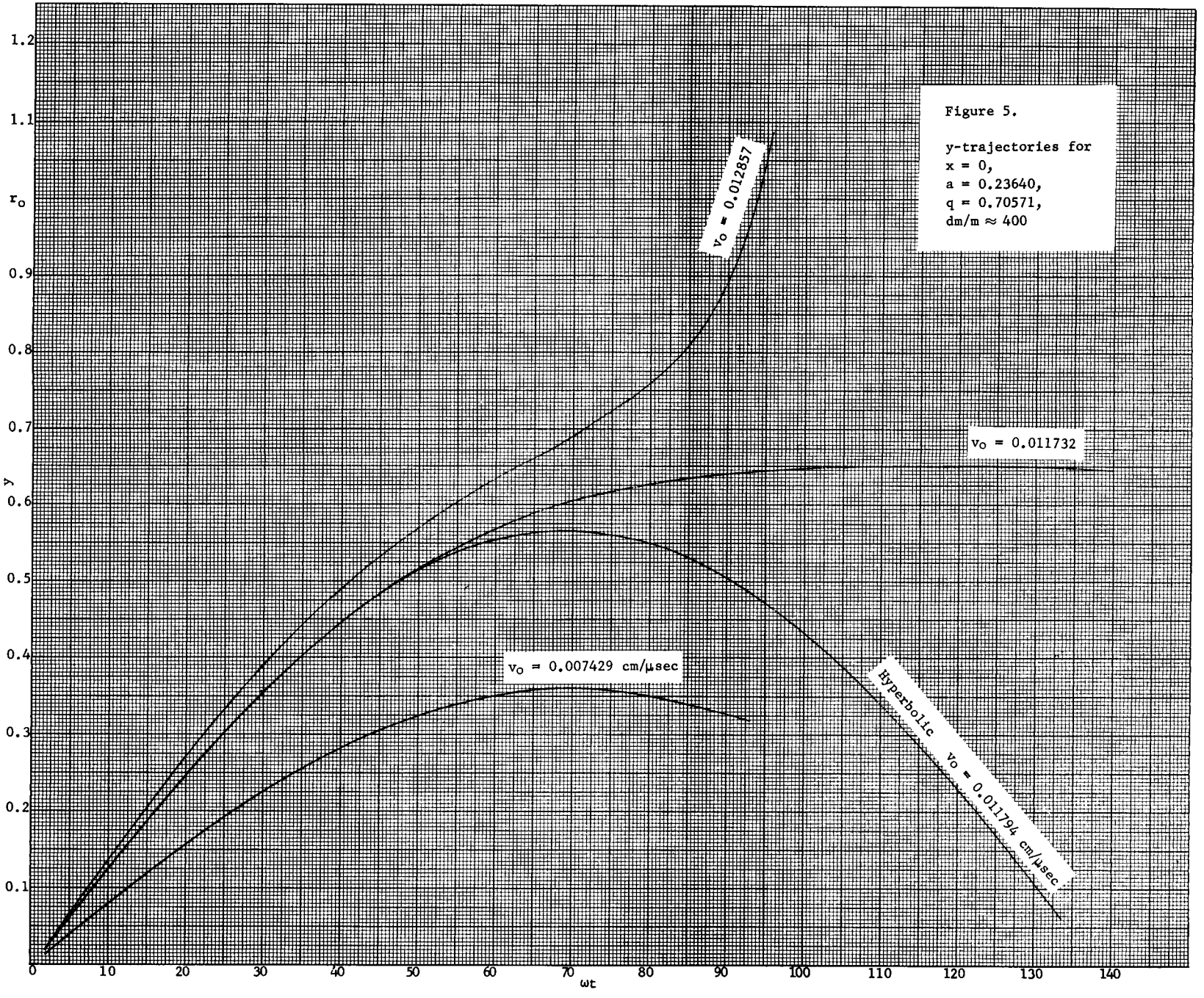
Figure 5.
y-trajectories for
x = 0,
a = 0.23640,
q = 0.70571,
dm/m ≈ 400
v_o = 0.012857
v_o = 0.011732
v_o = 0.007429 cm/μsec
Hyperbolic v_o = 0.011794 cm/μsec
r_o
y
ωt
1.2
1.1
0.9
0.8
0.7
0.6
0.5
0.4
0.3
0.2
0.1
0
10
20
30
40
50
60
70
80
90
100
110
120
130
140

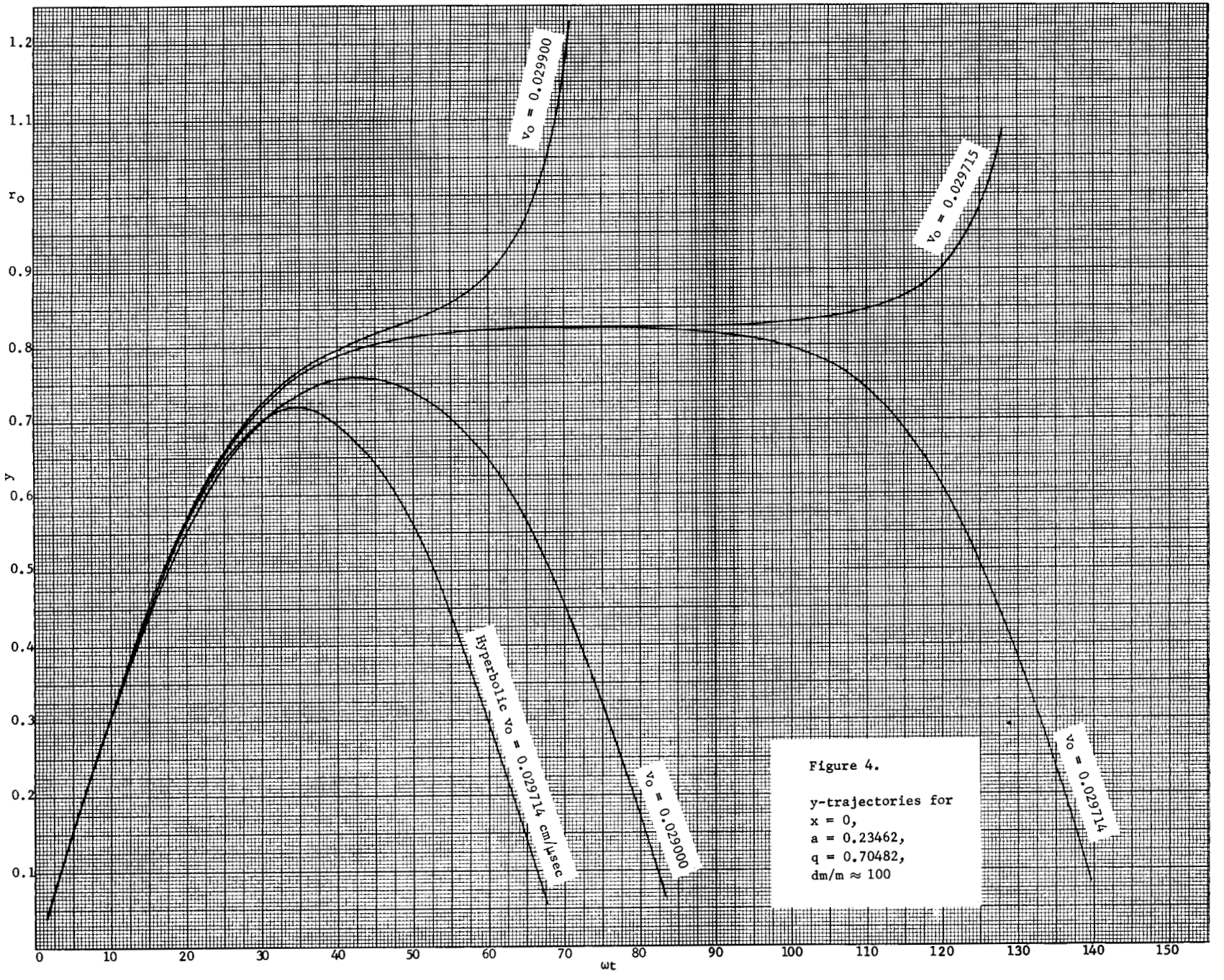

Figure 4.

y-trajectories for
x = 0,
a = 0.23462,
q = 0.70482,
dm/m ≈ 100

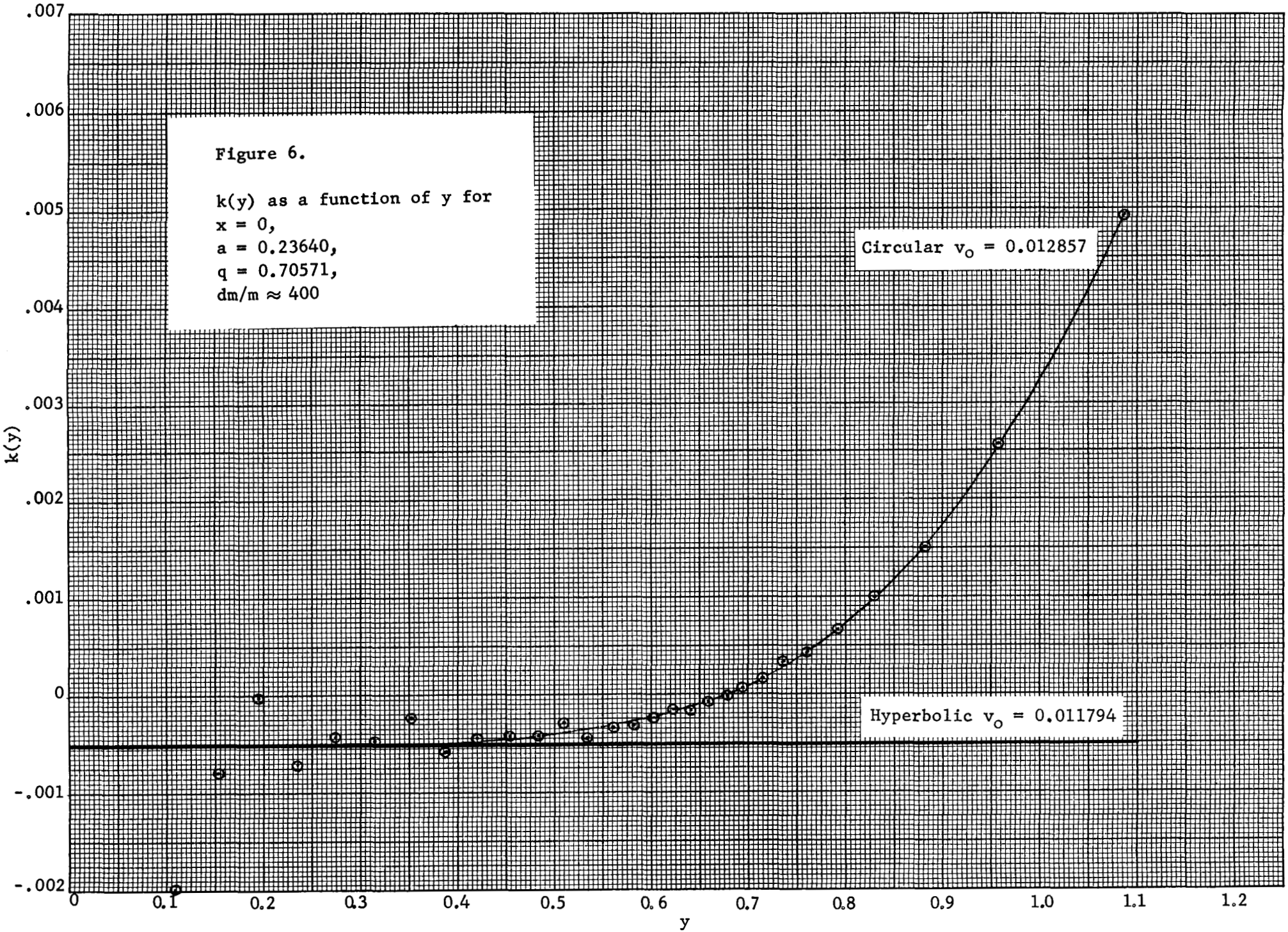
Figure 6.
k(y) as a function of y for
x = 0,
a = 0.23640,
q = 0.70571,
dm/m ≈ 400
Circular v_o = 0.012857
Hyperbolic v_o = 0.011794
k(y)
y
.007
.006
.005
.004
.003
.002
.001
0
-.001
-.002
0
0.1
0.2
0.3
0.4
0.5
0.6
0.7
0.8
0.9
1.0
1.1
1.2

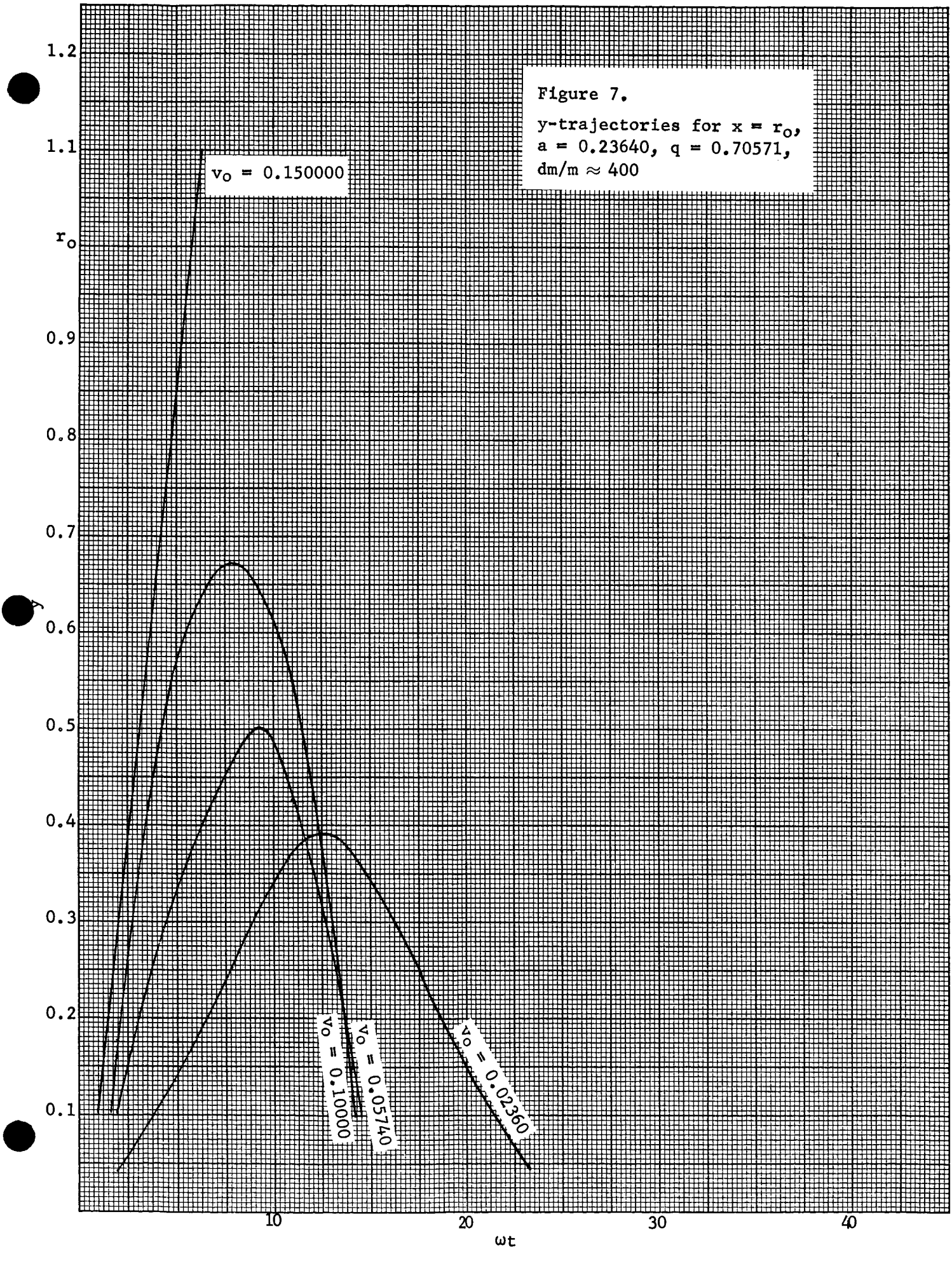

Figure 7.

y-trajectories for $x = r_o$, $a = 0.23640$, $q = 0.70571$, $dm/m \approx 400$

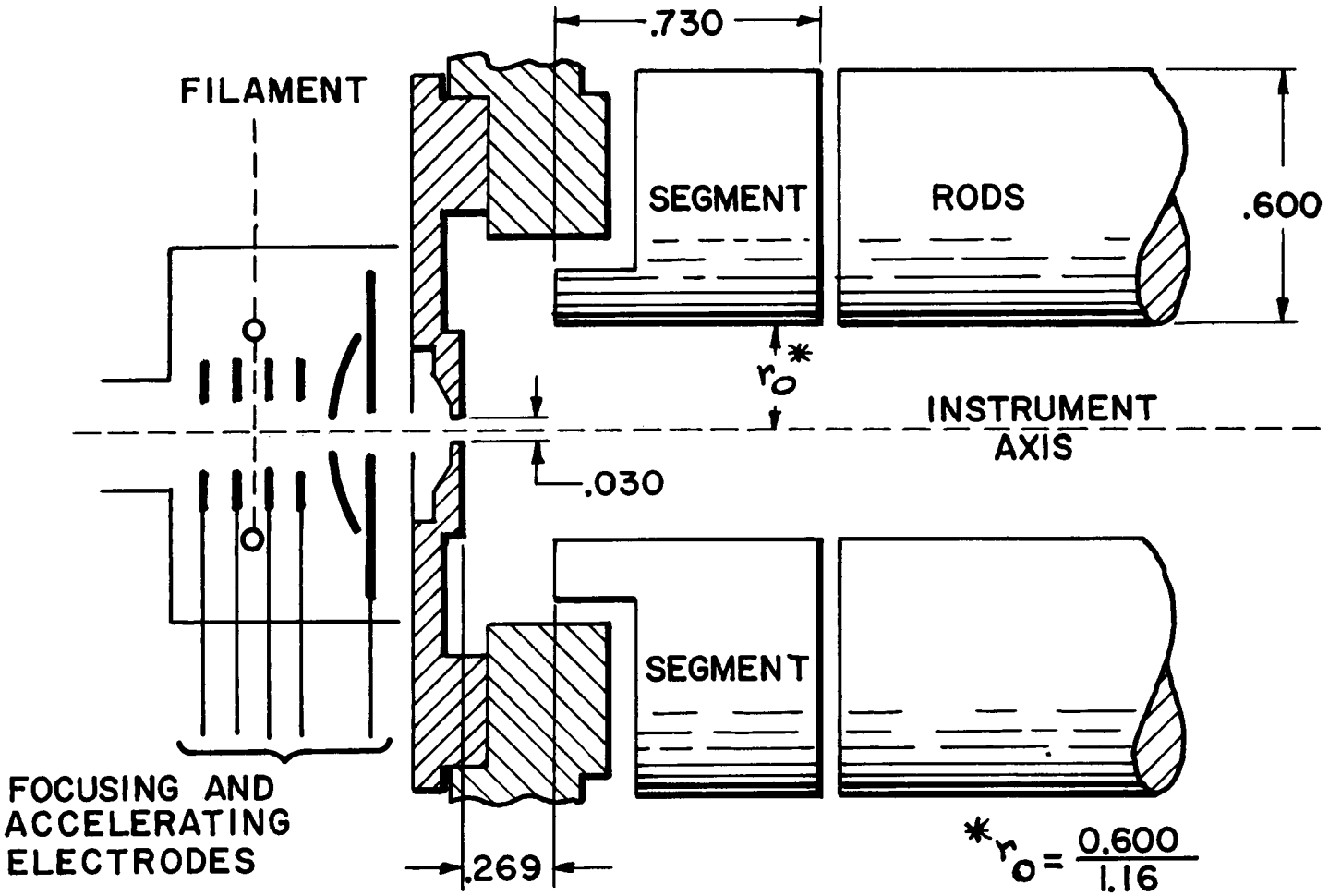

ION SOURCE & ENTRANCE GEOMETRY
FIGURE 8

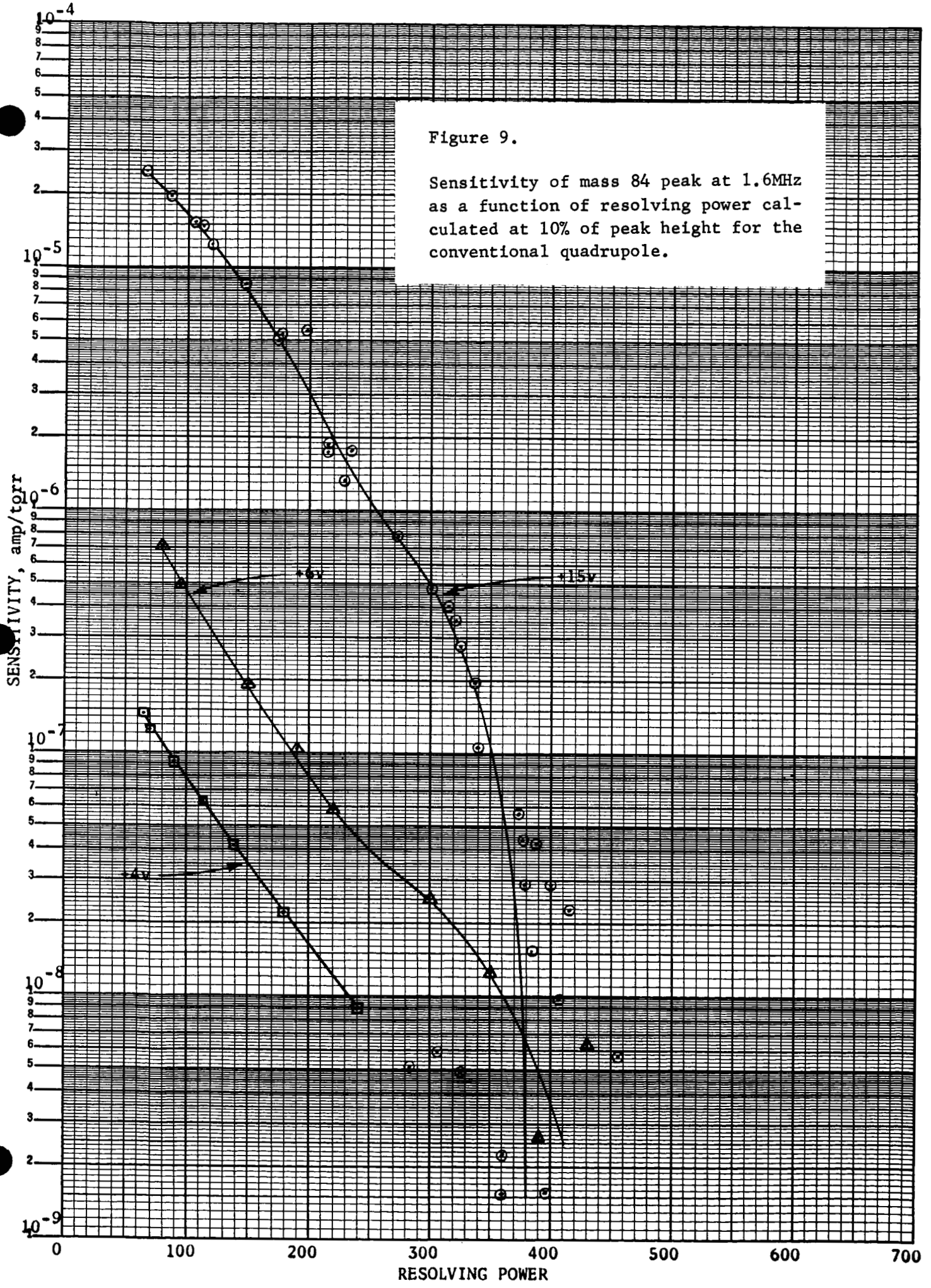

Figure 9.

Sensitivity of mass 84 peak at 1.6MHz as a function of resolving power calculated at 10% of peak height for the conventional quadrupole.

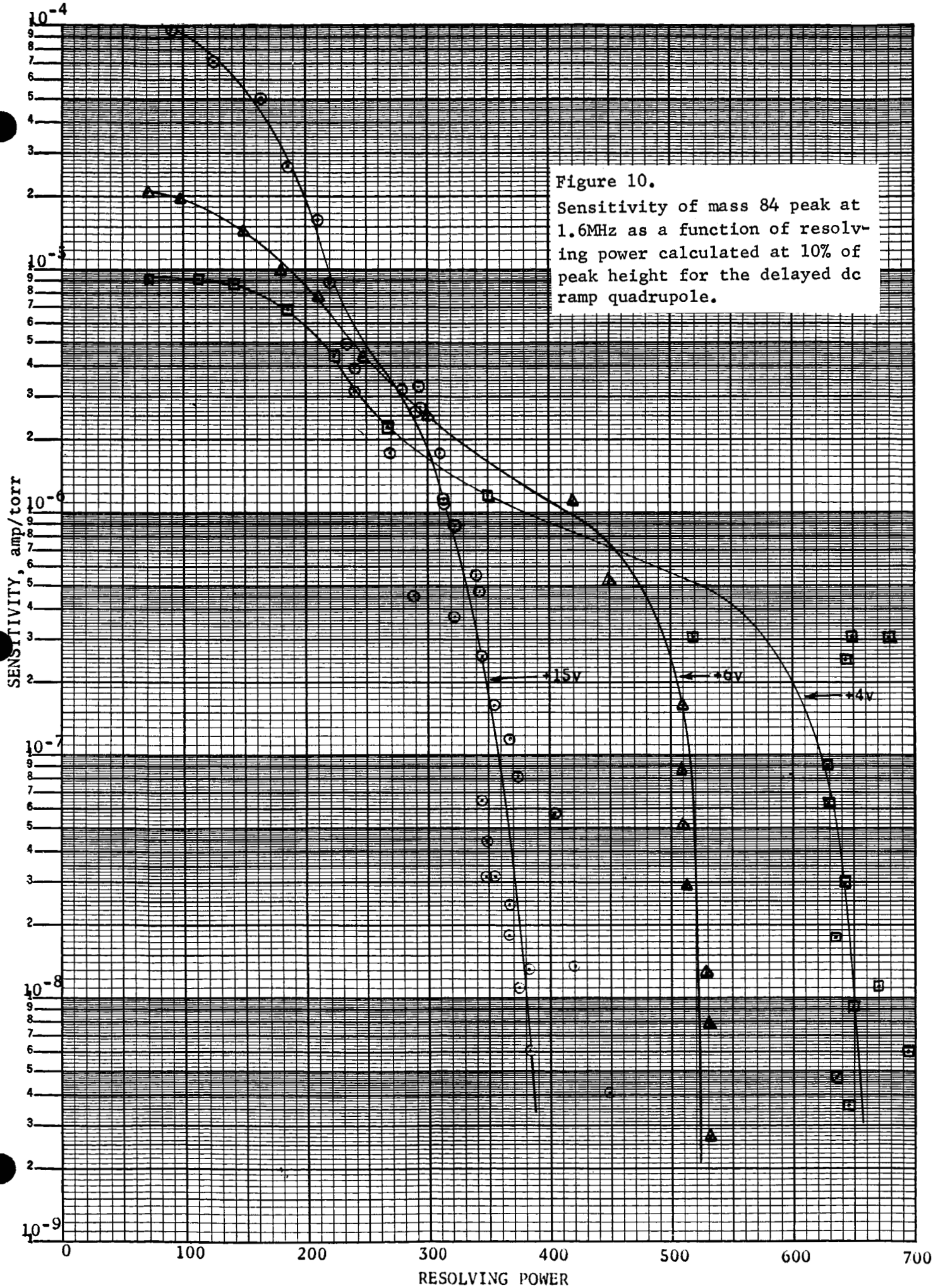

Figure 10.
Sensitivity of mass 84 peak at 1.6MHz as a function of resolving power calculated at 10% of peak height for the delayed dc ramp quadrupole.

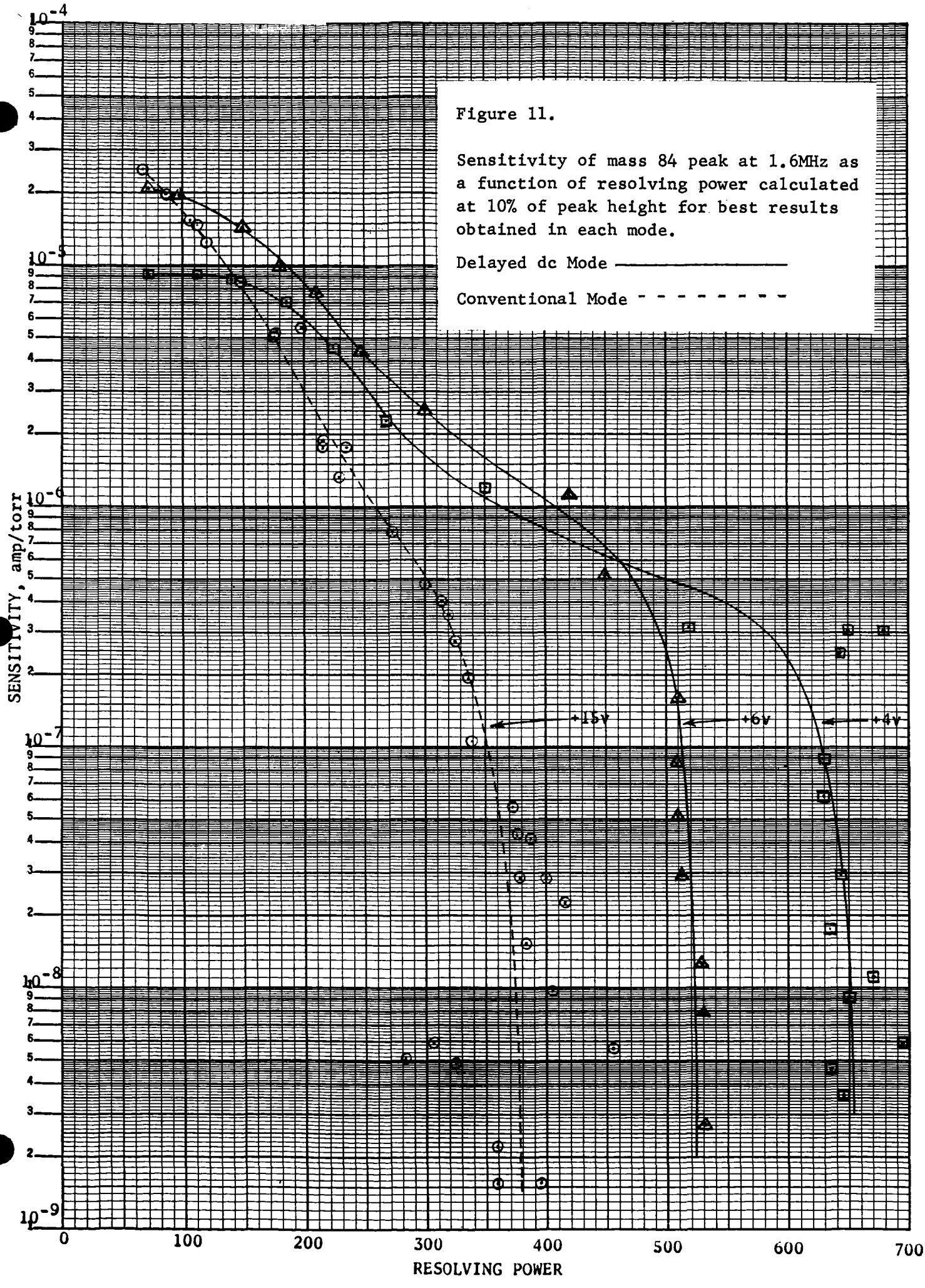

Figure 11.

Sensitivity of mass 84 peak at 1.6MHz as a function of resolving power calculated at 10% of peak height for best results obtained in each mode.

Delayed dc Mode ————————

Conventional Mode - - - - - - - -

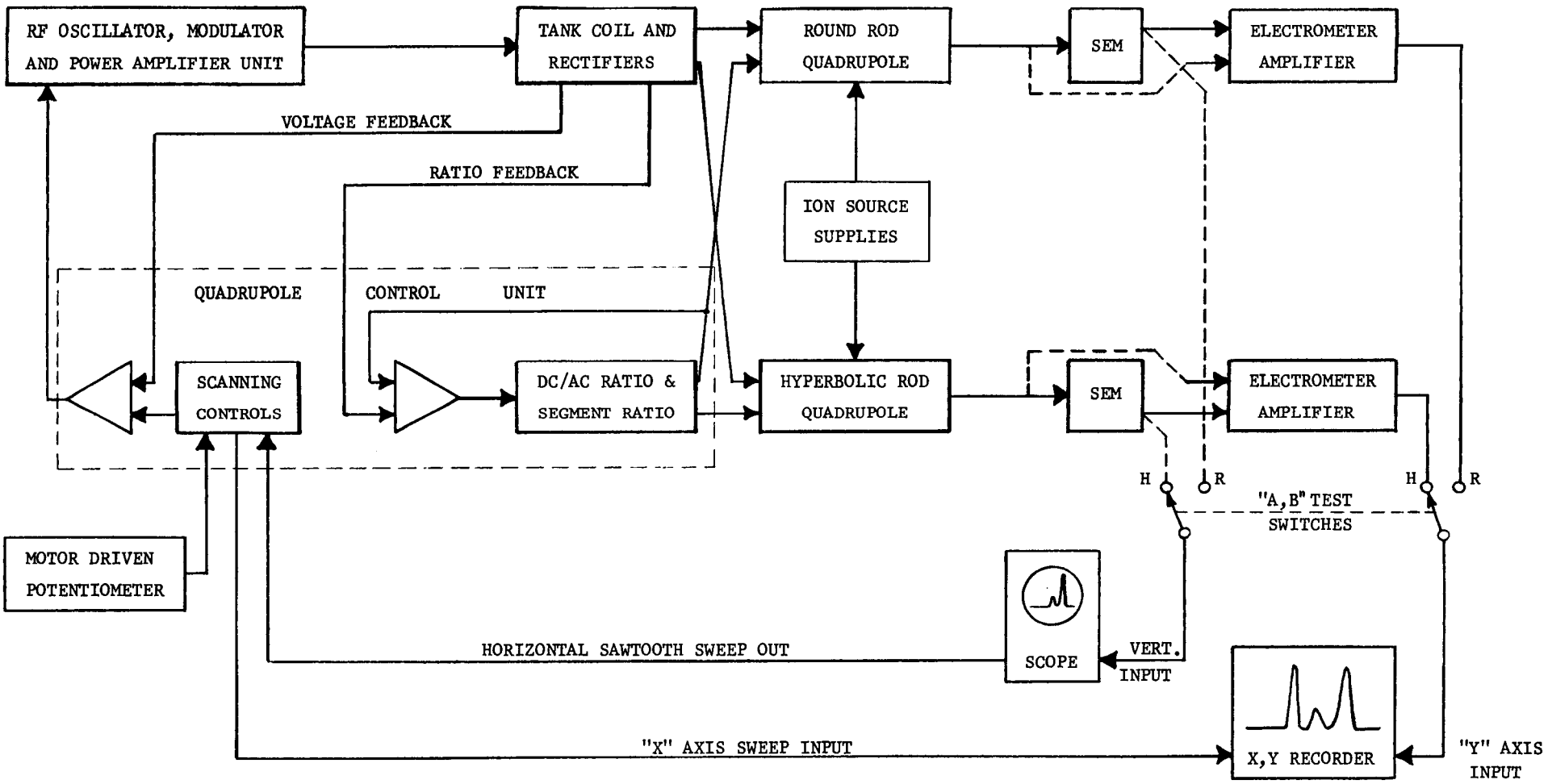

FIGURE 12

SIMPLIFIED BLOCK DIAGRAM OF NEW ELECTRONIC APPARATUS FOR COMPARISON OF

ROUND VERSUS HYPERBOLIC QUADRUPOLE RODS